LASERS

PACS numbers: 42.55.Ah; 42.60.Jf; 42.65.Es
DOI: 10.1070/QE2001v031n03ABEH001918

Numerical simulation of an SBS-mirror laser

V V Tumorin, E I Shklovskii

Abstract. **A three-dimensional mathematical model of a repetitively pulsed SBS-mirror laser is proposed, which describes the development of lasing, the interaction of counterpropagating beams in a saturated active medium, and the scattering of a focused beam in an SBS-active medium. Based on this model, the possibility of forming a laser mode of large volume with divergence close to the diffraction limit is shown. The factors that cause an increase in the transverse size of the laser mode are analysed.**

Keywords: *SBS-mirror laser, lasing-mode volume, phase conjugation quality.*

1. Introduction

Phase conjugation (PC) in stimulated Brillouin scattering (SBS) has long been used for correcting phase distortions and increasing radiation brightness in flashlamp-pumped solid-state laser systems employing the master oscillator – multipass amplifier scheme.

In recent years, new publications devoted to the analysis of operation of such systems have noticeably decreased in number. In our opinion, this is caused by the fact that flashlamp-pumped laser systems are gradually replaced by diode-pumped lasers. The characteristics of emission of diode-pumped solid-state lasers are considerably weaker affected by phase and polarisation distortions compared to flashlamp-pumped lasers, predominantly due to a weaker (by a factor of 10 – 20) heating of the active medium. However, in systems with high-power diode pumping, the heat release in the active medium, which is responsible for these distortions, becomes substantial. It is clear that the engineering solutions developed earlier for flashlamp-pumped lasers (Faraday rotators and PC based devices) will also find application in high-power pulsed diode-pumped lasers [1, 2]. On the other hand, nonlinear mirrors (including SRS mirrors) for the formation of the time pulse profile and the transformation of the spatial and frequency spectrum are already extensively used in diode-pumped lasers [3, 4].

V V Tumorin, E I Shklovskii General Physics Institute, ul. Vavilova 38, 119991 Moscow, Russia

Received 22 November 2000
Kvantovaya Elektronika **31** (3) 203 – 208 (2001)
Translated by A N Kirkin

It follows from the aforesaid that the study of specific features of operation of nonlinear mirrors in laser systems remains an urgent problem, the more so as some phenomena discovered during the period of an increased interest in SBS-mirror lasers have not been analysed in detail. Among such phenomena are an increase in the cross section of the fundamental mode of a laser oscillator with an external SBS mirror [5, 6].

An optical schematic of a Nd:YAG laser with an external SBS mirror is shown in Fig. 1. The laser cavity is formed by two mirrors, a cell with an SBS-active medium being placed behind one of these mirrors. As follows from experiments, the operation of this laser is particularly efficient when its mirrors have a low reflectivity, i.e., when lasing is developed under conditions of a relatively high energy stored in the active medium. Behind one of the mirrors, which represents a plane-parallel plate or a glass wedge, a cell with an SBS-active medium is placed. The second mirror represents either a glass etalon or a dielectric mirror with a reflectivity of 15 – 20 %. Thus, emission comes out from this 'starting' cavity predominantly in the direction of the SBS mirror.

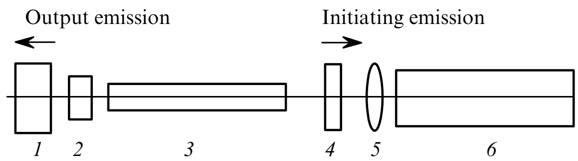

Figure 1. Optical schematic of a laser with an external SBS mirror: (*1*) glass etalon ($R \sim 15$ %); (*2*) passive switch; (*3*) Nd:YAG laser; (*4*) mirror ($R = 4 - 10$ %); (*5*) focusing lens; (*6*) SBS cell.

In experiments, conditions were realised when single-mode radiation was outcoupled from the starting cavity with a large Fresnel number in the absence of a selecting aperture. Such conditions are realised in lasers using heads with elliptic mirror illuminators, which concentrate pump radiation predominantly along the optical axis of a laser rod, and working near the threshold.

A LiF:F_2^- crystal was used in the starting cavity as a Q-switch. Note that a method by which a single-mode initiating signal is formed is likely to be of minor importance. One can use for this purpose standard methods, for instance, a telescope in a cavity, Gaussian mirrors, and other optical elements that favour lasing on a mode with a smooth spatial profile (even of small cross section).

To produce lasing in a cavity formed by the front mirror and the SBS mirror, an initiating signal is needed to obtain a sufficiently high reflectivity of a nonlinear medium. The subsequent lasing dynamics is mainly determined by the time-dependent parameters of this cavity. Note that the output radiation mode (Fig. 1) is nearly Gaussian and fills almost the entire volume of a laser rod.

An increase in the mode cross section in a laser with an external SBS mirror can be explained either by the enhancement of wings of the transverse distribution or by the inaccuracy of phase conjugation of multifrequency pump radiation, which leads to the broadening of the directivity diagram of radiation reflected from the SBS cell [7, 8]. As far as we know, only a single paper [9] is available in which the operation of the given scheme is analysed from the viewpoint of the possibility of increasing the width of the beam of broad band radiation reflected from the SBS mirror. However, the mathematical model used there is unable to give a complete picture of processes occurring in the laser.

Here, we make an attempt to simulate the operation of a pulsed Nd:YAG laser with an external SBS mirror and determine on the basis of our model its spatial and time characteristics and the factors that affect an increase in the mode volume.

2. Mathematical model

We use a three-dimensional mathematical model of an SBS-mirror laser, which describes the development of lasing in the starting cavity with a passive Q-switch and stimulated scattering of the focused pump beam in an SBS-active medium. The calculations were made in the approximation of axial symmetry. In this case, the radiation field in the cavity is written in the form

$$E = A_1(z, r, t)\exp(\mathrm{i}\omega_0 t - \mathrm{i}kz) + A_2(z, r, t)\exp(\mathrm{i}\omega_0 t + \mathrm{i}kz),$$

where A_1 and A_2 are slowly varying amplitudes of counterpropagating waves and ω_0 is the initiating-radiation frequency.

All information on the frequency and spatial radiation spectrum is contained in the field amplitude $A(z, r, t)$. Because emission of an SBS-mirror laser contains field components with the frequencies ω_0, $\omega_0 - \Omega$, $\omega_0 - 2\Omega$, ... (Ω is the Stokes frequency shift in an SBS-active medium), this imposes limitations on the step of the calculation grid along the axes t and z:

$$\Delta t = \frac{\Delta z}{c} \ll \frac{2\pi}{n\Omega}, \tag{1}$$

where $n \approx 4$ is the assumed number of Stokes components in laser emission. For liquids, the Stokes shift is about 0.1 cm^{-1}, and therefore the grid step Δz proves to be considerably smaller than the typical distance between the elements of the laser system, which requires storing of large data bases.

To calculate changes in the transverse amplitude distribution of the wave travelling between optical elements of the system, we used direct and inverse Fourier transforms in the axially symmetric case and took into account the phase incursion for different spatial components of the field.

The interaction of counterpropagating waves on the saturated-gain grating of a homogeneously broadened active laser medium is described by the system of equations [10]

$$\frac{n}{c}\frac{\partial A_1}{\partial t} + \frac{\partial A_1}{\partial z} + \frac{\mathrm{i}}{2k}\Delta_\perp A_1 = \frac{1}{2}(1 - \mathrm{i}\delta)(A_1 g_0 + A_2 g_1),$$

$$\frac{n}{c}\frac{\partial A_2}{\partial t} - \frac{\partial A_2}{\partial z} + \frac{\mathrm{i}}{2k}\Delta_\perp A_2 = \frac{1}{2}(1 - \mathrm{i}\delta)(A_2 g_0 + A_1 g_1^*),$$

$$T_1\frac{\partial g_0}{\partial t} + (g_0 - a_0) \tag{2}$$

$$= -(A_1A_1^* + A_2A_2^*)g_0 - A_1A_2^*g_1 - A_1^*A_2g_1,$$

$$T_1\frac{\partial g_1}{\partial t} + g_1 = -(A_1A_1^* + A_2A_2^*)g_1 - A_1A_2^*g_0,$$

where the squares of field amplitudes are normalised to the saturation intensity of the active medium; g_0 and g_1 are the first and second terms of the expansion of gain $g(z, r, t)$ of the active medium in spatial frequencies along the z-axis; $a_0(r)$ is the gain formed by the external pump radiation; $\delta = (w - w_0)T_2$ is the frequency detuning of the wave relative to the gain line centre; $T_2 = 1.6$ ps is the polarisation relaxation time of the active medium of the Nd:YAG laser; and $T_1 = 250$ μs is its population relaxation time.

The initial gain distribution over the cross section of the active element was specified by the function $a_0(r) = a_{0\mathrm{m}}\{1 + h[\exp(-r^2/r_0^2) - 1]\}$. To describe the gain distribution in the active element 4 mm in diameter in a standard K-301 laser head, the quantities h and r_0 were set equal to 0.15 and 1.7 mm, respectively.

The effect of saturated-absorption gratings in a passive Q-switch based on a medium with a large transition cross section manifests itself only at the initial stage of formation of a Q-switched pulse. Because of this, the Q-switch transmission was calculated in the approximation of an infinitely thin two-level saturable medium:

$$T_\mathrm{s}(r, t) = \exp(-n),$$

$$\tau_\mathrm{s}\frac{\mathrm{d}n}{\mathrm{d}t} + n - n_0 = -\frac{(A_1A_1^* + A_2A_2^*)(1 - T_\mathrm{s})}{I_\mathrm{s}}, \tag{3}$$

where T_s is the transmission coefficient of the passive switch; n is the density of population difference in the switch normalised to σ^{-1}; σ is the transition cross section; n_0 is the initial population difference; τ_s is the relaxation time of the absorbing medium; and I_s is its saturation intensity. Nonresonant losses in the passive switch were modelled by placing two absorbers on both sides of the switch.

The fundamental mode of the starting cavity was found by injecting there weak initiating radiation with the Gaussian field distribution over the beam section. After a certain number of round trips of initiating radiation in the cavity, a stationary field distribution corresponding to the desired cavity mode was formed. Our numerical experiments show that the nonuniformity of gain over the cross section of the active element, which was described above, lead to a rapid selection of the fundamental transverse cavity mode that occupies a small volume of the active medium.

When the power of initiating radiation incident on the SBS mirror exceeded 0.1 of the threshold SBS power, we applied the model of the SBS mirror, which describes the nonstationary scattering of the pump beam focused into the SBS-active medium. The system of equations describing the interaction of pump ($A_p(z,r,t)\exp(i\omega_p t - ik_p z)$) and Stokes ($A_s(z,r,t)\exp(i\omega_s t + ik_s z)$) waves with oscillations of the medium in the approximation of a small hypersound damping length has the form

$$-\frac{n}{c}\frac{dA_s^*}{dt}+\frac{\partial A_s^*}{\partial z}+\frac{i}{2k}\Delta_\perp A_s^*+\frac{g}{2}\rho^* A_p=0,$$
$$\frac{n}{c}\frac{dA_p}{dt}+\frac{\partial A_p}{\partial z}+\frac{i}{2k}\Delta_\perp A_p+\frac{g}{2}\rho A_s^*=0, \quad (4)$$
$$T_r\frac{\partial\rho}{\partial t}+\rho=A_pA_s+F_n(z,r,t),$$

where g is the SBS gain; ρ is the hypersound density; T_r is the hypersound relaxation time; and F_n is the noise function of thermal perturbations.

In the cylindrical coordinate system, the Laplacians entering in the equations have the form

$$\Delta_\perp A=\frac{\partial^2 A}{\partial r^2}+\frac{1}{r}\frac{\partial A}{\partial r}. \quad (5)$$

In the case of tight focusing of a Gaussian beam into an SBS-active medium, the field amplitude and the hypersound density are conveniently represented in the form

$$A=\frac{A'}{q}\exp\left(\frac{-ikr^2}{2q}\right),$$
$$\rho=\frac{\rho'}{|q|^2}, \quad (6)$$

where $q=i|q_0|+z$ is the complex parameter of the Gaussian beam; $|q_0|=kw_0^2/2$ and w_0 are the length and the width of the waist of the Gaussian beam, respectively.

Making a change to the curvilinear coordinate system fixed to the Gaussian beam

$$r=\frac{w_0}{2}r'\left[1+\tan^2(z')\right]^{1/2},$$
$$z=|q_0|\tan(z'), \quad (7)$$
$$t=n|q_0|t'/c,$$

we obtain the system of equations

$$-\frac{1}{\cos^2 z'}\frac{dA_s'^*}{dt'}+\frac{\partial A_s'^*}{\partial z'}+i\frac{\partial^2 A_s'^*}{\partial r'^2}+i\frac{\partial A_s'^*}{\partial r'}\left(\frac{1}{r'}-r'\right)$$
$$+\frac{g'}{2}\rho^* A_p'=0,$$
$$\frac{1}{\cos^2 z'}\frac{dA_p'}{dt'}+\frac{\partial A_p'}{\partial z'}+i\frac{\partial^2 A_p'}{\partial r'2}+i\frac{\partial A_p'}{\partial r'}\left(\frac{1}{r'}-r'\right)$$
$$+\frac{g'}{2}\rho A_s'^*=0, \quad (8)$$
$$T_r'\frac{\partial\rho'}{\partial t'}+\rho'=A_p'A_s'\exp\left(-\frac{r'^2}{2}\right)+F_n(z',r',t'),$$
$$0\leqslant r'\leqslant r'_{max}, \quad -\frac{\pi}{2}\leqslant z'\leqslant\frac{\pi}{2},$$

where $g'=g/|q_0|$.

We took into account the Stokes frequency shift Ω when matching the amplitudes $A_s'(z'=-\pi/2,r',t)$ and $A_2(z_{sbs},r,t)$:

$$A_2(z_{sbs},r,t)=A_{th}A_s'\left(z'=-\frac{\pi}{2},r'=\frac{2r}{W},t\right)$$
$$\times\exp\left(-i\Omega t-\frac{r^2}{W^2}\right), \quad (9)$$
$$A_p\left(z'=-\frac{\pi}{2},r',t\right)=\frac{1}{A_{th}}A_1\left(z_{sbs},r=\frac{r'W}{2},t\right)\exp\left(\frac{r^2}{W^2}\right),$$

where A_{th} is the threshold field amplitude at the centre of the Gaussian pump beam with the half-width W. For this field amplitude normalisation, the SBS gain is $g'=2M/\pi$ ($M\approx 21$ is the threshold gain increment for the Stokes wave).

System of equations (8) was solved for the following boundary conditions:

$$\frac{\partial^2 A'_{s,p}(z',r'=r'_{max},t)}{\partial r'^2}=0,$$
$$A_s'\left(z'=\frac{\pi}{2},r',t\right)=0. \quad (10)$$

To weaken the effect of the boundary of the calculation region $r'=r'_{max}$, we introduced additional radiation absorption in the region $0.9r'_{max}<r'<r'_{max}$.

To obtain a stable difference scheme when solving the system of differential equations, the increments of real and imaginary parts of field amplitudes were calculated sequentially and, when finding the hypersound density, we averaged the product $A_p'A_s'$ over two neighbouring points along the z axis with different weight coefficients. In this case, the stability of the difference grid was obtained for $\Delta z'(\Delta r')^{-2}<1$, where $\Delta z'$ and $\Delta r'$ are the grid steps along the coordinates z' and r'. For $r'_{max}>8$, the modified amplitudes of pump and Stokes waves at the boundary of the calculation region may reach considerable values, which leads to calculation errors. Because of this, we set $r'_{max}\leqslant 7.5$ in the calculations.

3. Calculation results

In the numerical experiment, we simulated a laser system with the starting cavity 58 cm long. The output cavity mirror represented a glass etalon 3.6 cm thick with a maximum reflectivity of 16 %. The reflectivity of the cavity mirror positioned on the side of the SBS mirror was taken equal to 4 %. The remaining parameters of the laser system were as follows: the saturation energy of the active medium was 0.5 J cm^{-2}, the initial transmittance of the passive switch $T_{s0}=0.4$, the saturated transmittance of the passive switch $T_s=0.8$, the relaxation time of hypersound in the SBS-active medium (CCl_4) $T_r=1$ ns, the Stokes shift $\Omega=2.7$ GHz, the threshold excitation power of the SBS mirror $A_{th}^2\pi W^2/2=400$ kW, and the interaction length of counterpropagating waves in the SBS-active medium was 10 cm.

Fig. 2 presents transverse intensity distributions in the beam of initiating radiation of the starting cavity for the blocked SBS mirror at the initial stage of development of a giant pulse and the energy density distribution over the beam cross section in a Q-switched pulse for different focal distances of the thermal lens induced in the active element by pump radiation.

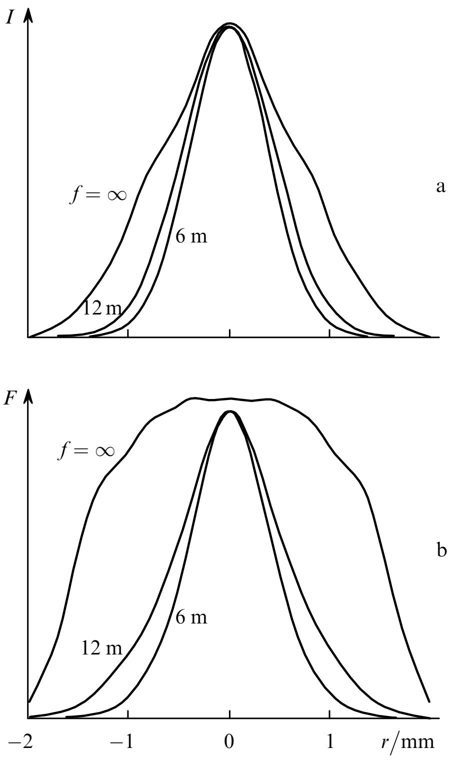

Figure 2. Initial intensity distribution (a) and the energy density distribution of a giant pulse (b) over the cross section of the beam of initiating emission for different focal distances f of the thermal lens in the active element.

As mentioned above, the fundamental cavity mode was selected owing to the nonuniformity of gain over the cross section of the active element. In this case, at the initial lasing stage, an excess over the threshold is achieved only for a narrow region near the axis of the active element. In the case of a plane-parallel cavity and the absence of a thermal lens in the active element, this leads to the formation of a small-volume initial mode. The development of lasing, the bleaching of a sufficiently dense passive switch, and the saturation of gain in the active element are accompanied by a substantial increase in the volume of the lasing mode.

The divergence of the resulting large-volume mode is close to the diffraction limit. However, to realise this scheme in practice, one should use a high-quality active element and exactly compensate for the thermal lens induced in the active element in a laser working in the repetitively pulsed mode.

In a stable starting cavity (with accounting for the thermal lens in the active element), the transverse field distribution of initiating radiation is close to the mode of the passive cavity and undergoes considerably weaker changes during the giant-pulse generation. This case is of considerable interest for practice and, therefore, further numerical experiments were carried out for a stable starting cavity.

The excitation of the SBS mirror by an initiating radiation pulse switches the system to the regenerative-amplification mode. The total energy reflectivity obtained for the SBS mirror in the numerical experiments without accounting for loss through radiation absorption in the SBS medium was about 90 %. Because of this, the Q-factor of the cavity with the SBS mirror was substantially higher than the Q-factor of the starting cavity, which provided obtaining output radiation pulses with energy above 100 mJ in the calculation.

In practice, the energy reflectivity of the SBS mirror in laser systems of this kind is lower (60 – 80 %) because of the self-action of the pump beam in an absorbing SBS-active medium [11] and the development of SBS and optical breakdown, which compete with SRS and manifest themselves with increasing power of nonstationary pump radiation incident on the SBS mirror. As a result, the output radiation energy in the actual laser system whose parameters were used in the numerical model reaches only 60 mJ [6].

The time structure of the output emission contains several peaks corresponding to Stokes pulses of different orders. Owing to the adaptive properties of the SBS mirror, the lasing mode is no longer determined by the stability of the starting cavity. In the course of laser radiation formation, the intensity of the amplified emission is redistributed over the beam cross section and the highest gain is obtained for the peripheral beam regions (Fig. 3). In particular, the radiation of the third Stokes pulse, which has an annular intensity distribution, completely fills the aperture of the active element.

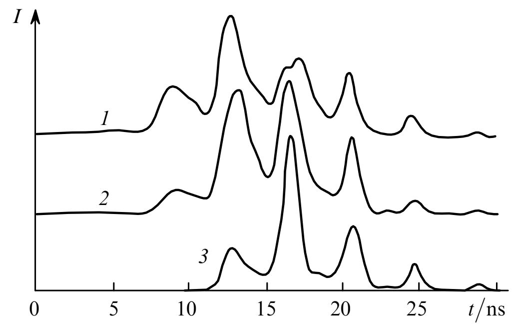

Figure 3. Time dependence of the output beam intensity at the center of the active element (*1*) and at distances of 1 (*2*) and 1.5 mm (*3*) for the 3-m focal distance of the thermal lens in the active medium.

Note that a nearly one-mode distribution of the energy density over the cross section of the output beam (Fig. 4a) is caused by a superposition of beams corresponding to different cavity round trips. In this case, the intensity distributions in the beams corresponding to different round trips may have different profiles, including the annular one (Fig. 5).

According to the calculated data, an increase of the transverse distribution of the amplified emission in width is accompanied by a decrease of its divergence. In particular, the integrated divergence of the output radiation pulse at a level of 0.1 exceeds the diffraction limit only by a factor of 1.3 – 1.5 (Fig. 4b). However, the experimental data obtained in [6] show that the output radiation has a somewhat higher divergence in comparison with the initiating radiation. It is likely that the difference of experimental and calculated data may be caused by the influence of the aforementioned processes competing with SBS and by the self-focusing of high-power laser radiation in a laser rod.

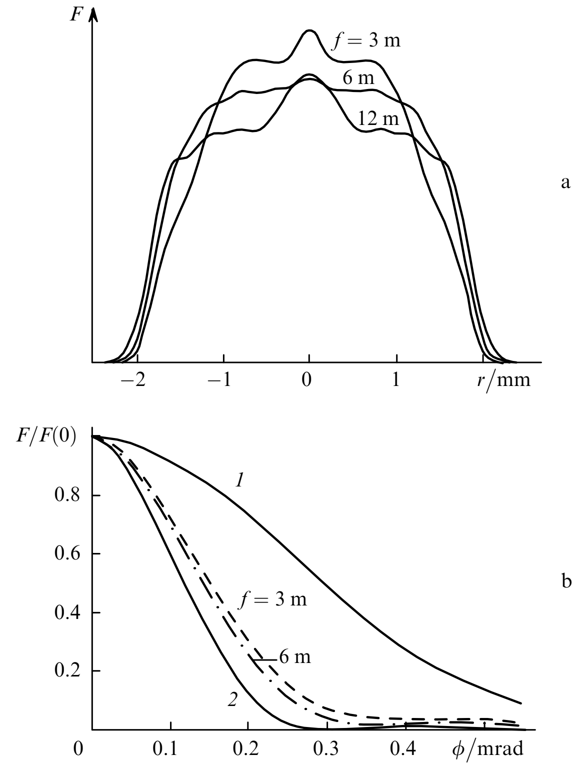

Figure 4. Transverse distributions of energy density in the near-field (a) and far-field (b) regions of the output beam for different focal distances f of the thermal lens in the active element and the energy density distributions for the initiating emission (*1*) and the plane wave diffracted by the aperture of the active element (*2*).

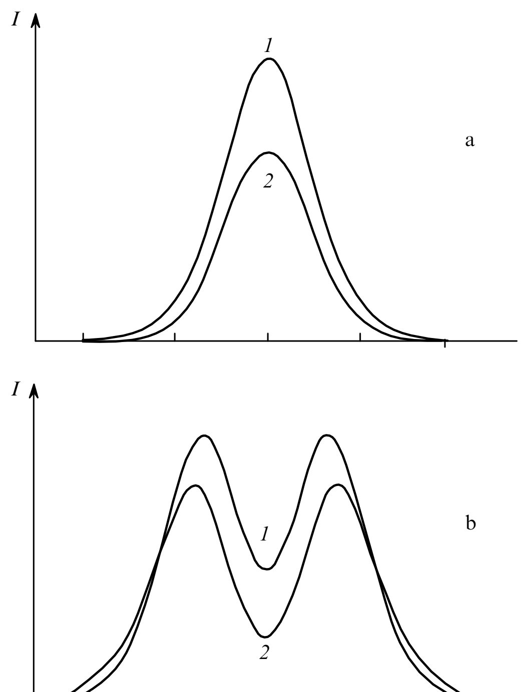

Figure 5. Transverse intensity distribution in the incident beam (*1*) and the beam reflected from the SBS mirror (*2*) for the first (a) and third (b) round trips of the amplified emission in the cavity.

To estimate the phase conjugation quality, we used in the calculations the parameter η', which was defined by the expression

$$\eta' = \frac{\int\left|\int A_{\mathrm{p}} A_{\mathrm{s}} \mathrm{d}S\right| \mathrm{d}t}{\int\left(\int |A_{\mathrm{p}}|^2 \mathrm{d}S \int |A_{\mathrm{s}}|^2 \mathrm{d}S\right)^{1/2} \mathrm{d}t}. \tag{11}$$

We have intentionally departed from the commonly accepted definition of the PC quality parameter η [11, 12] for a more adequate description of PC for nonstationary pump radiation.

The value of the parameter $\eta' = 0.95$ obtained in the numerical experiment in which an isolated pulse of one-mode single-frequency radiation was incident on the SBS mirror agrees with the results of Ref. [12]. For the SBS mirror working in the laser scheme, the calculated value of the parameter η' decreased down to 0.85 – 0.89. This is primarily caused by the fact that each subsequent Stokes pulse is excited after the end of generation of the preceding pulse. Therefore, at certain moments of time, the two-frequency pump radiation with frequencies ω_0 and $\omega_0 - \Omega$ or $\omega_0 - \Omega$ and $\omega_0 - 2\Omega$, or $\omega_0 - 2\Omega$ and $\omega_0 - 3\Omega$, etc. is incident on the SBS mirror.

However, because the time intervals in which two neighboring modes in the numerical experiment produced beatings at the input of the SBS mirror were short and a small hypersound relaxation time (1 ns) caused a rapid tuning of the SBS-mirror grating to a new frequency of incident radiation, the deviation of the PC quality parameter from the ideal value was small. It is likely that the same cause accounts for the fact that the numerical experiments showed no substantial increase in the width of the scattered beam relative to the incident one (Fig. 5) that is typical of PC for SBS of wide-band pump radiation [8].

A high PC quality accompanied by a rather exact reproduction of the transverse structure of the beam reflected from the SBS mirror shows that an increase in the laser mode volume, which was obtained in the calculations, cannot be explained by specific features of operation of the SBS mirror. We made a numerical experiment in which the model of an 'ideal' PC mirror with $\eta = 1$ was used. The reflectivity of this mirror at each moment of time was calculated by using the SBS mirror model described above. The data obtained in this experiment for the energy of output radiation and its distribution in the near-field region agree with an error of 7 % with the results obtained above.

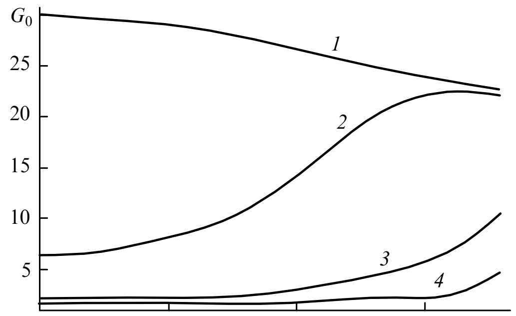

Figure 6. Distribution of small-signal gain along the radius of the active element at the initial moment of time (*1*) and after the passage of the first (*2*), second (*3*), and third (*4*) Stokes radiation pulses.

At the same time, the gain of the active element is substantially saturated in the course of lasing, especially in the central beam regions (Fig. 6). Even for the second Stokes pulse, the gain at the center of the active element becomes lower than the losses in the cavity formed by the output and SBS mirrors, which inevitably leads to a preferential amplification of peripheral beam regions on the second and third cavity round trips. These data suggest that the saturation of gain in the active element is the dominant mechanism of an increase in laser mode volume in an SBS-mirror laser in the case of a strong modulation of the Q-factor of the laser cavity.

4. Conclusions

The mathematical model presented for an SBS-mirror laser gives a satisfactory agreement between the calculated and the experimental data [6]. However, some effects observed in the experiment, such as a decrease in the width of the transverse distribution of output radiation with increasing distance from the starting cavity to the SBS mirror and an increase in divergence of the output radiation with respect to the divergence of initiating radiation cannot be adequately described from the positions of the given mathematical model taking into account only SBS. For a better description of SBS-mirror lasers, one should take into account such nonlinear optical phenomena as self-focusing of radiation and the processes competing with SBS (in particular, SRS).

Acknowledgements. The authors thank N N Il'ichev for the useful discussion of the results. This work was supported by the Russian Foundation for Basic Research (Grants Nos 97-02-17397 and 98-02-17498).

References

1. Ho J G, St.Pierre R, Morais J, Poylio J, Long W, Weber M, Valley M M *Technical Digest of the Conference on Advanced Solid-State Lasers* (Davos, 2000, paper MA4-1) p. 9
2. Herman M, Honig J, Hackel L *Proceedings of the Conference on Lasers and Electro-Optics* (OSA Tech. Digest series, 1995, Vol. 15) p. 61
3. Lagatsky A A, Abdolvand A, Kuleshov N V *Opt. Lett.* **25** 616 (2000)
4. Findeisen J, Eichler H J, Penser P *Opt. Commun.* **181** 129 (2000)
5. Pashinin P P, Shklovskii E I *Kvantovaya Elektron.* **15** 1905 (1988) [*Quantum Electron.* **18** 1190 (1988)]
6. Voskoboinik E V, Pashinin P P, Sidorin V S, Shklovskii E I *Kvantovaya Elektron.* **22** 242 (1995) [*Quantum Electron.* **25** 226 (1995)]
7. Kochemasov G G, Nikolaev V D *Kvantovaya Elektron.* **4** 115 (1977) [*Sov. J. Quantum Electron.* **7** 60 (1977)]
8. Glazkov D A, Gordeev A A, Zubarev I G, Mikhailov S I *Kvantovaya Elektron.* **19** 286 (1992) [*Sov. J. Quantum Electron.* **22** 262 (1992)]
9. Kir'yanov A V, Aboites V, Il'ichev N N *J. Opt. Soc. Am. B* **17** 11 (2000)
10. Bel'dyugin I M, Stepanov A A, Shcheglov V A *Kratk. Soobshch. Fiz. FIAN* No. 9 40 (1986)
11. Kir'yanov Yu F, Kochemasov G G, Maslov N V *Kvantovaya Elektron.* **25** 61 (1998) [*Quantum Electron.* **28** 58 (1998)]
12. Kir'yanov Yu F, Kochemasov G G, Maslov N V, Shestakova I V *Kvantovaya Elektron.* **18** 588 (1991) [*Sov. J. Quantum Electron.* **21** 533 (1991)]